INTERNATIONAL ATOMIC ENERGY AGENCY
UNITED NATIONS EDUCATIONAL, SCIENTIFIC AND CULTURAL ORGANIZATION
INTERNATIONAL CENTRE FOR THEORETICAL PHYSICS
I.C.T.P., P.O. BOX 586, 34100 TRIESTE, ITALY, CABLE: CENTRATOM TRIESTE

SMR.755/23

Workshop on Fluid Mechanics

(7 - 25 March 1994)

The main geomagnetic field and its secular variations

J.-L. Le Mouël
Laboratoire de Sismologie
Institut de Physique du Globe
4, Place Jussieu
75252 Paris Cedex 05
France

Le noyau

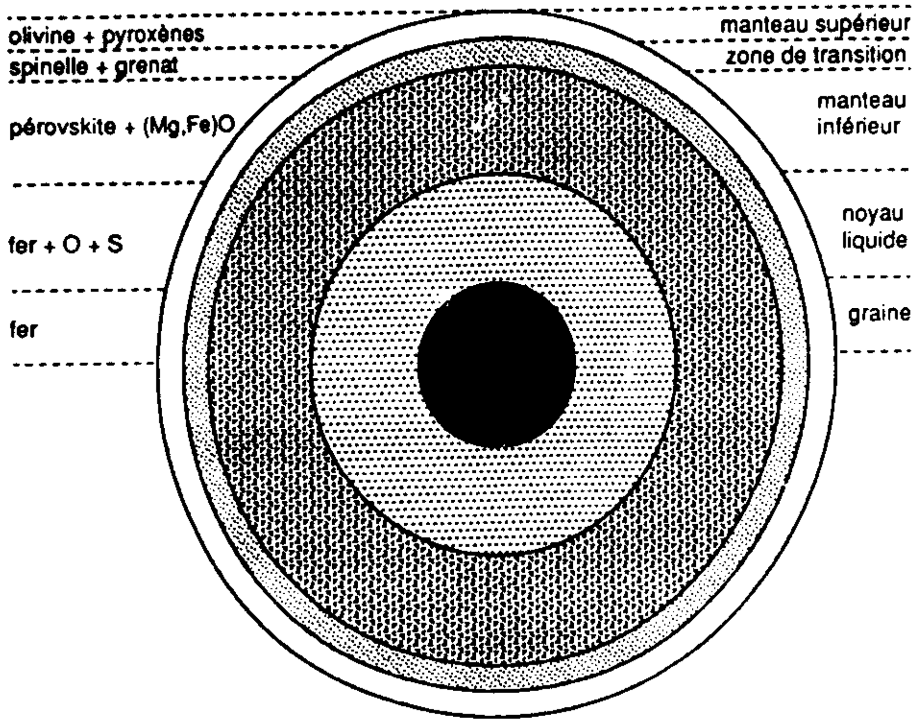

Fig. 3-10 : *La Terre minéralogique.*
Ce schéma, à l'échelle, résume la constitution minéralogique (simplifiée) des principales régions de l'intérieur de la Terre. La croûte n'est pas représentée.

(Mg, Fe) SiO$_3$ 80% perovskite

(Mg, Fe) O 20% magnésiowustite

Modèles de composition

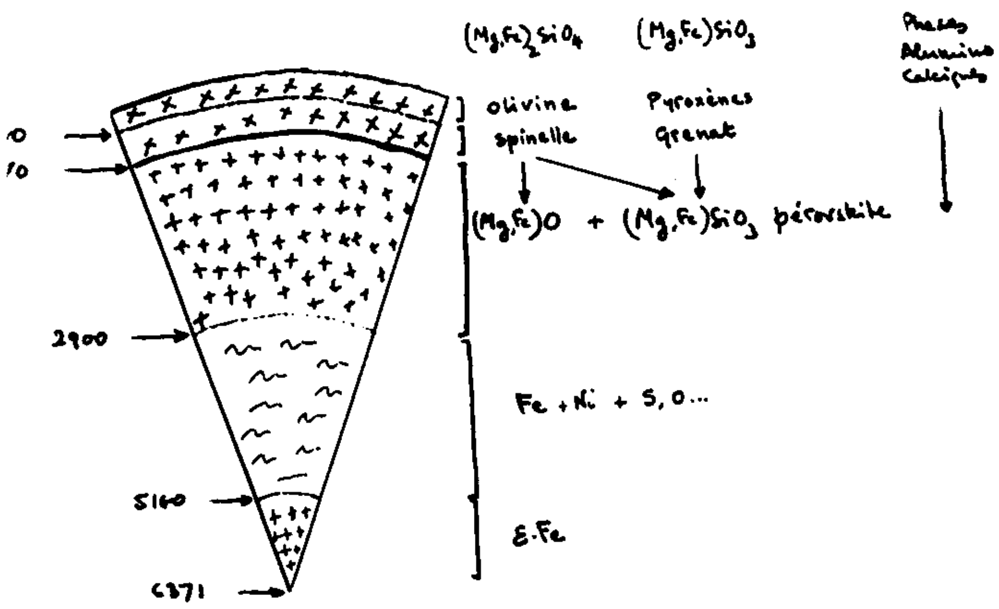

Modèles fournis par la sismologie

$$V(r) = \sqrt{\frac{k_s + (4/3)\mu}{\rho}}$$

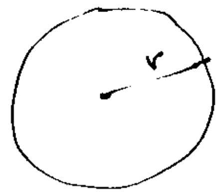

$$W(r) = \sqrt{\frac{\mu}{\rho}}$$

$$k_S^{-1} = -\frac{1}{v}\left(\frac{\partial v}{\partial p}\right)_S = \frac{1}{\rho}\left(\frac{\partial \rho}{\partial p}\right)_S$$

La sismologie $\longrightarrow$

$$\frac{K_s}{\rho} = \varphi(r) = V^2 - \frac{4}{3}W^2$$

Puis, l'hypothèse hydrostatique $\longrightarrow$

$$\frac{dp}{dz} = -\rho g \quad \left\{ \begin{array}{l} \longrightarrow \dfrac{d\rho}{dz} = g\rho/\varphi \\ g(r) = \dfrac{G}{r^2}\displaystyle\int_0^r 4\pi r^2 \rho(r)\, dz \end{array} \right.$$

Méthode d'Adams et Williamson (1923)

(suppose grad. adiab.)

Aujourd'hui :

Love, Raileigh, $_mS_n$, $_mT_n$

$\longrightarrow V(r), W(r), \rho(r)$

Loi de Birch dans le manteau supérieur. [illegible]

Birch | D. W

[illegible]

: $v_p = -1,87 + 3,05\rho$

$v_p = a + b\rho$

On se fixe la densité à la base de la croûte 3,3 c

à la base du manteau

et celle du fond du dessus

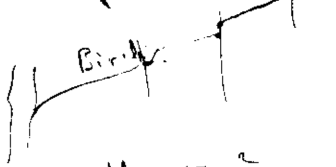

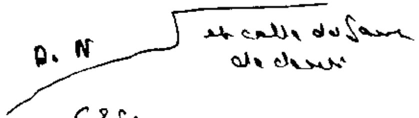

M, Ma²

6350
3900
5150

PREM

Dziewonski & Anderson, 1981

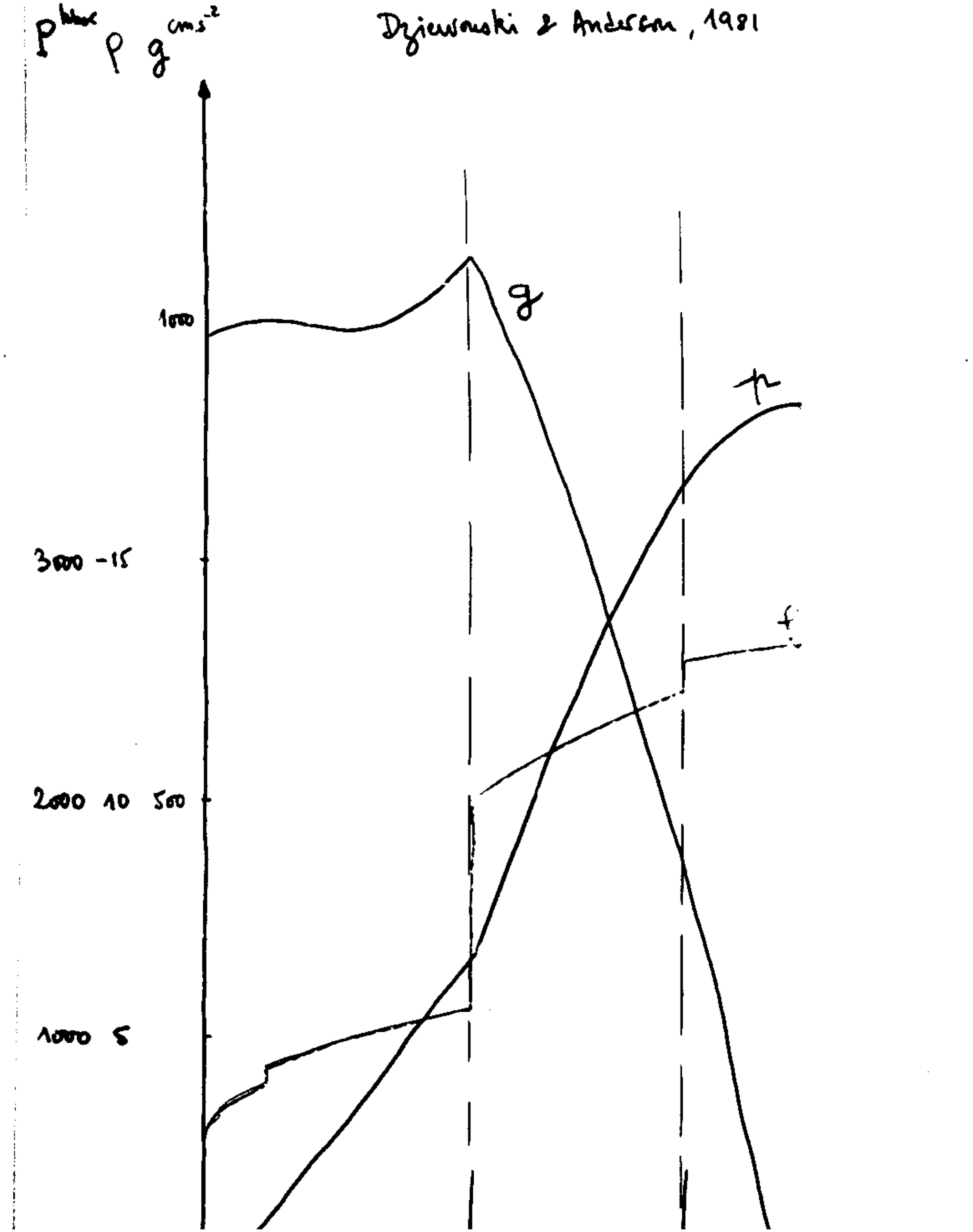

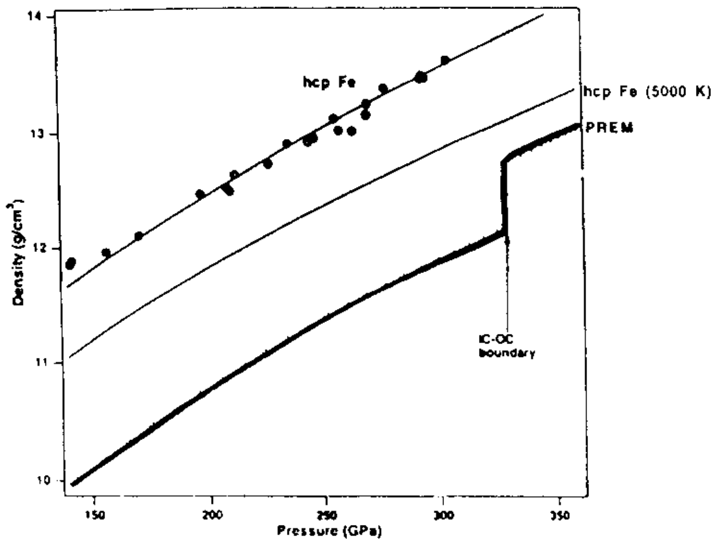

Geotherm T(r)

Temperature profiles are anchored on the seismic discontinuities which are identified with phase changes for which the relation (T, P) is known (experimentally or extrapolated:

A) inner core - outer core boundary: T_f

B) 670 km discontinuity: post spinel transition

$P \rightarrow T$

Between these anchoring points the temperature gradient is supposed to be adiabatic.

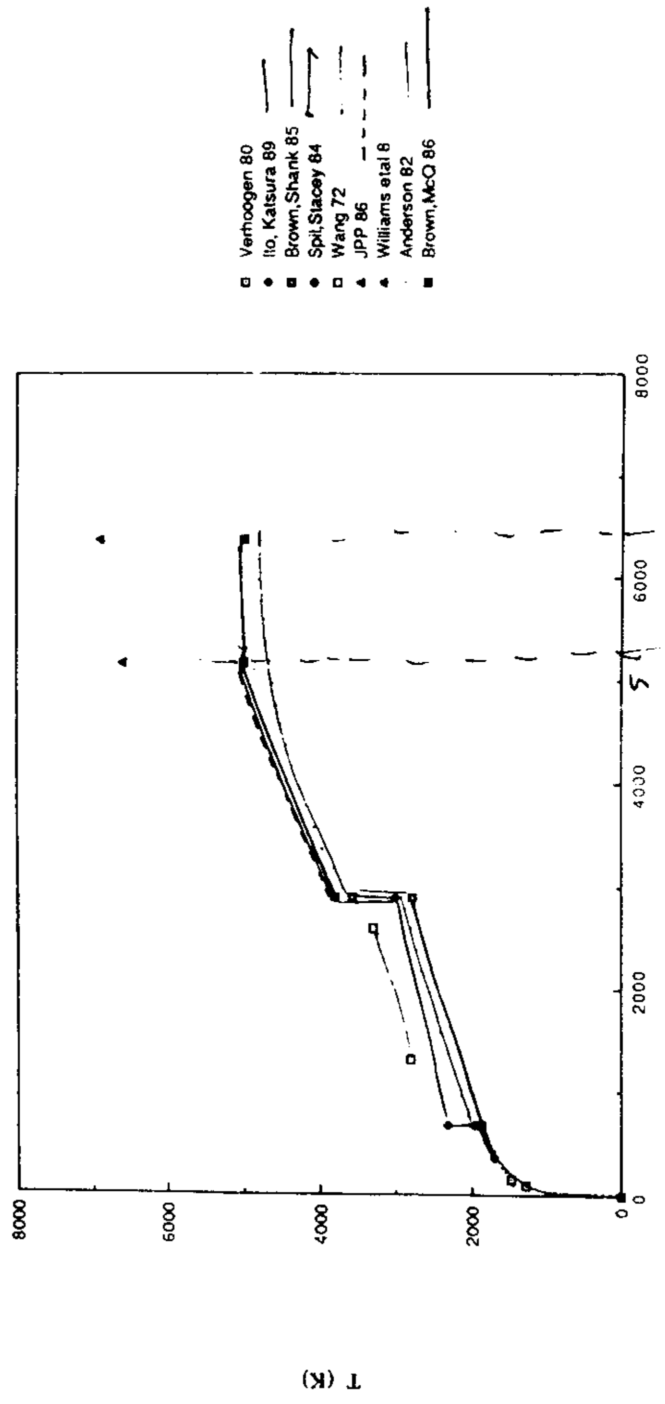

$T_c \sim 5000°$ K

Incertitude of 100 to 1000° or

Deep mantle conductivity

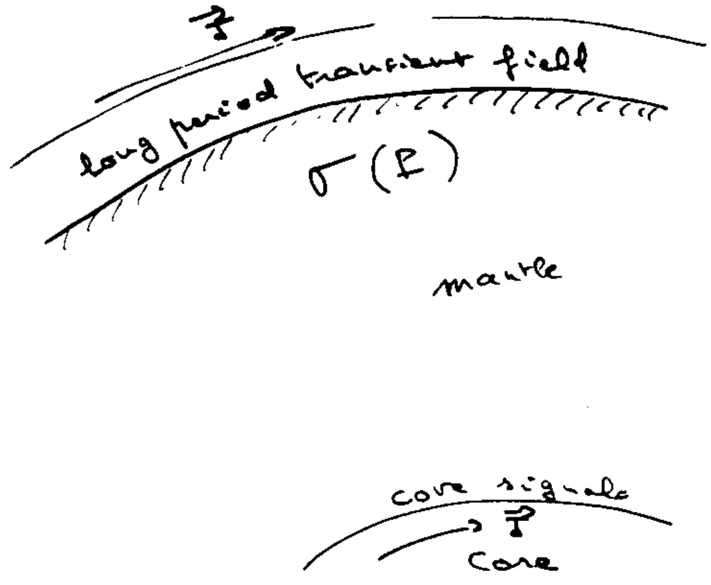

External signals : 24 hours and its harmonics
27 jours -- (...)
6 months
1 year
11 years and its harmonics

→ informations on σ down to 1500 km

Internal signals : short period changes of the main field.

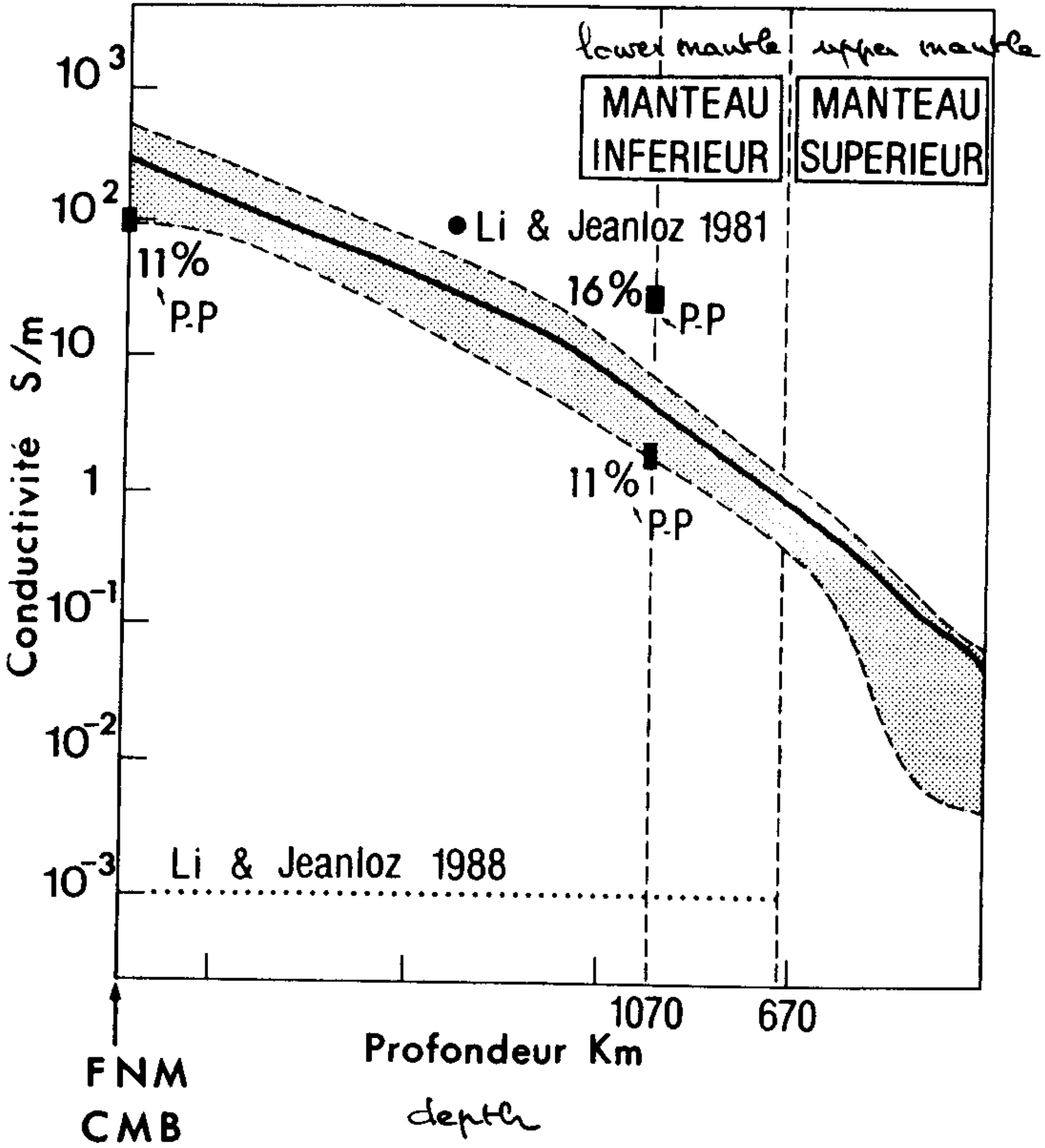

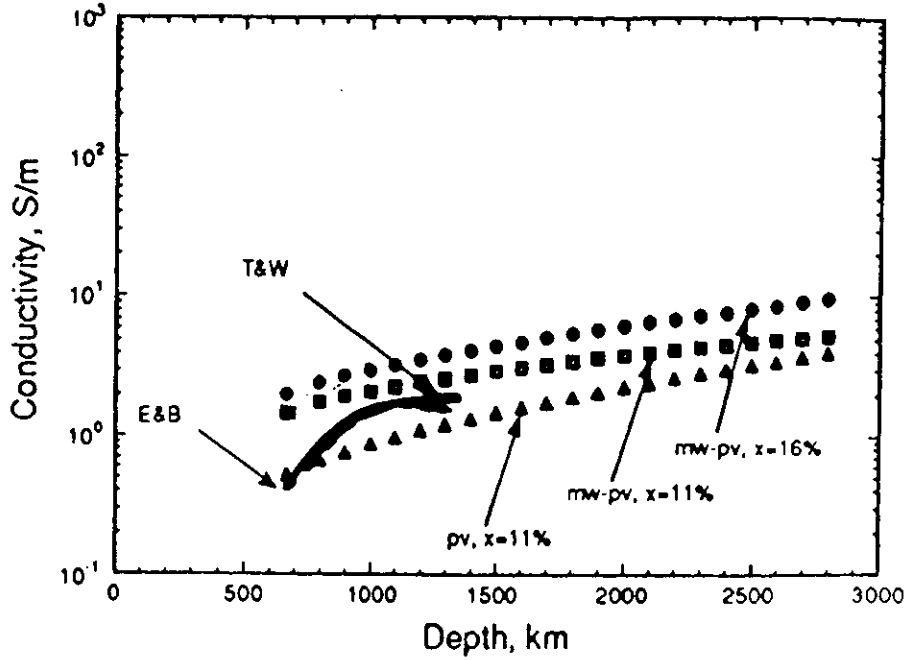

P.P : Peyronneau & Poirier 1991

II. The main geomagnetic field.

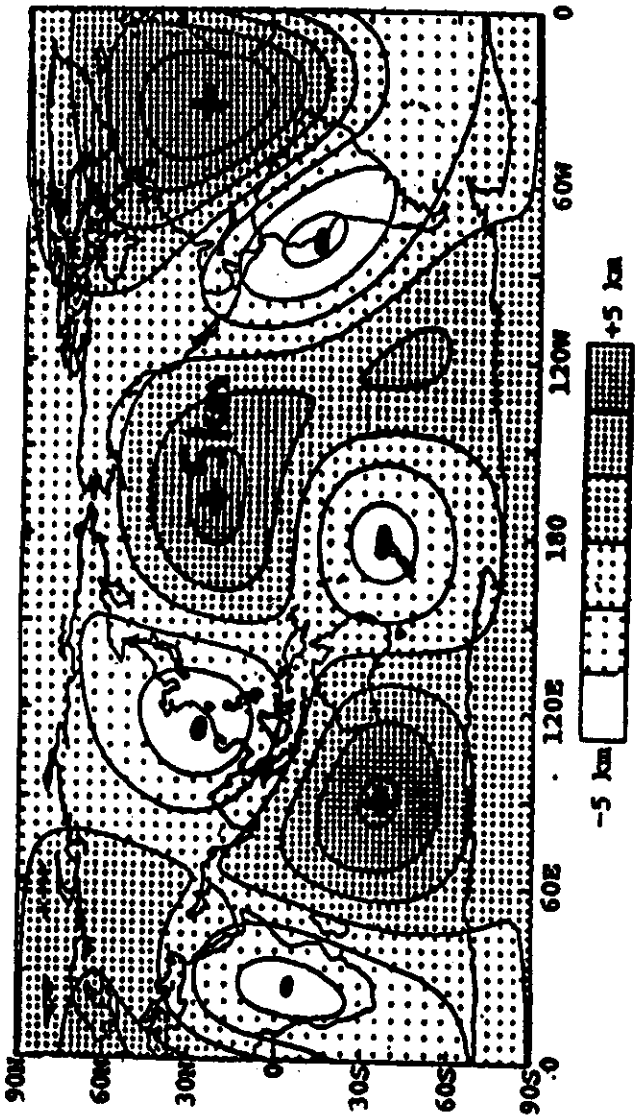

CMB topography
with respect to the hydrostatic ellipsoid

Topographie de Morelli et Dziewonski
(Harvard)

generated by electrical currents in the liquid outer core : the geodynamo

à l'extérieur de la Terre ($r \geq a$):
outside the Earth:

$$\sigma = 0 \qquad \vec{J} = 0 \longrightarrow \begin{array}{l} \mathrm{rot}\,\vec{B} = \nabla\times\vec{B} = 0 \\ \mathrm{div}\,\vec{B} = 0 \end{array}$$

the domain $r \geq a$
is simply connected: $\longrightarrow$

$$\begin{cases} \vec{B} = -\vec{\nabla} V \\ \nabla^2 V = 0 \end{cases}$$

$V(P,t)$ is the geomagnetic potential.

t : time

$P(x,y,z)$ or r,θ,φ

(r,θ,φ): geocentric spherical coordinates

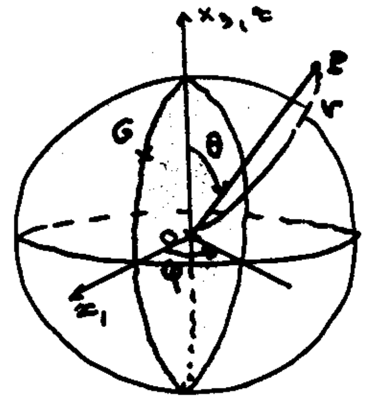

$P(r,\theta,\varphi)$

$$V(P,t) = a \sum_{n=1}^{\infty} \sum_{m=0}^{n} \left(\frac{a}{r}\right)^{n+1} \left[g_n^m(t)\, Y_n^{mc}(\theta,\varphi) + h_n^m(t)\, Y_n^{ms}(\theta,\varphi) \right]$$

g_n^m, h_n^m : Gauss coefficients in nT (10^{-9} tesla)

$$Y_n^{mc}(\theta,\varphi) = P_n^m(\cos\theta)\cos m\varphi$$

$$Y_n^{ms}(\theta,\varphi) = P_n^m(\cos\theta)\sin m\varphi$$

$P_n^m(\cos\theta)$: associate Legendre function of first kind.

Schmidt's normalisation:

$$\iint_{(r=1)} \left(Y_n^{m\,c,s}\right)^2 dS = \frac{4\pi}{2n+1}$$

Secular variation.

$$\dot{\vec{B}}(P,t) = \frac{\partial \vec{B}(P,t)}{\partial t}$$

$$\dot{\vec{B}} = a \sum_{n=1}^{\infty} \sum_{m=0}^{n} \left(\frac{a}{r}\right)^{n+1} \left[\dot{g}_n^m(t)\cos m\varphi + \dot{h}_n^m(t)\sin m\varphi \right] \times P_n^m(\cos\theta)$$

$$\dot{g}_n^m(t) = \frac{d g_n^m(t)}{dt}, \qquad \dot{h}_n^m(t) = \frac{d h_n^m(t)}{dt}$$

Orders of magnitude

$g_1^0 \sim 31\,000$ nT

$\dot{g}_1^0 \sim 20$ nT/year en 1980

Spectra. on the sphere of radius r.

$$W(r) = \frac{1}{4\pi r^2} \iint_{S(r)} \vec{B}^2\, dS = \sum_n W_n(r)$$

$$W_n(r) = \left(\frac{a}{r}\right)^{2(n+2)} (n+1) \sum_{m=0} \left[(g_n^m)^2 + (h_n^m)^2\right]$$

(with Shmidt's normalisation.)

Table 2. Coefficients of SV GSFC 80 and IGRF 80 models (up to degree 6).

GSFC 80				IGRF 80	
n	m	$\dot{g}_n^m$	$\dot{h}_n^m$	$\dot{g}_n^m$	$\dot{h}_n^m$
1	0	20.51		22.4	
1	1	9.08	−9.04	11.3	−15.9
2	0	−19.53		−18.3	
2	1	4.78	−18.74	3.2	−12.7
2	2	9.86	−26.82	7.0	−25.2
3	0	4.51		0.0	
3	1	−3.55	−5.57	−6.5	0.2
3	2	−2.19	1.64	−0.7	2.7
3	3	3.87	−6.62	1.0	−7.9
4	0	−2.20		−1.4	
4	1	−2.24	3.66	−1.4	4.6
4	2	−10.09	1.08	−8.2	1.6
4	3	−3.82	6.77	−1.8	2.9
4	4	−5.54	−2.73	−5.0	0.4
5	0	−1 04		1.5	
5	1	−0.86	3.30	0.4	1.3
5	2	−0.73	0.50	−0.8	−0.4
5	3	−4.81	−0.82	−3.3	0.0
5	4	0.11	1.09	0.2	1.3
5	5	1.49	0.87	1.4	2.1
6	0	0.75		0.4	
6	1	−0.04	0.03	0.0	−0.5
6	2	3.49	−1.20	3.4	−1.4
6	3	2.20	−0.96	0.8	0.0
6	4	0.44	0.11	0.8	−1.6
6	5	1.78	0.56	0.3	0.5
6	6	1.34	2.72	−0.1	0.0

$W_n(a)$

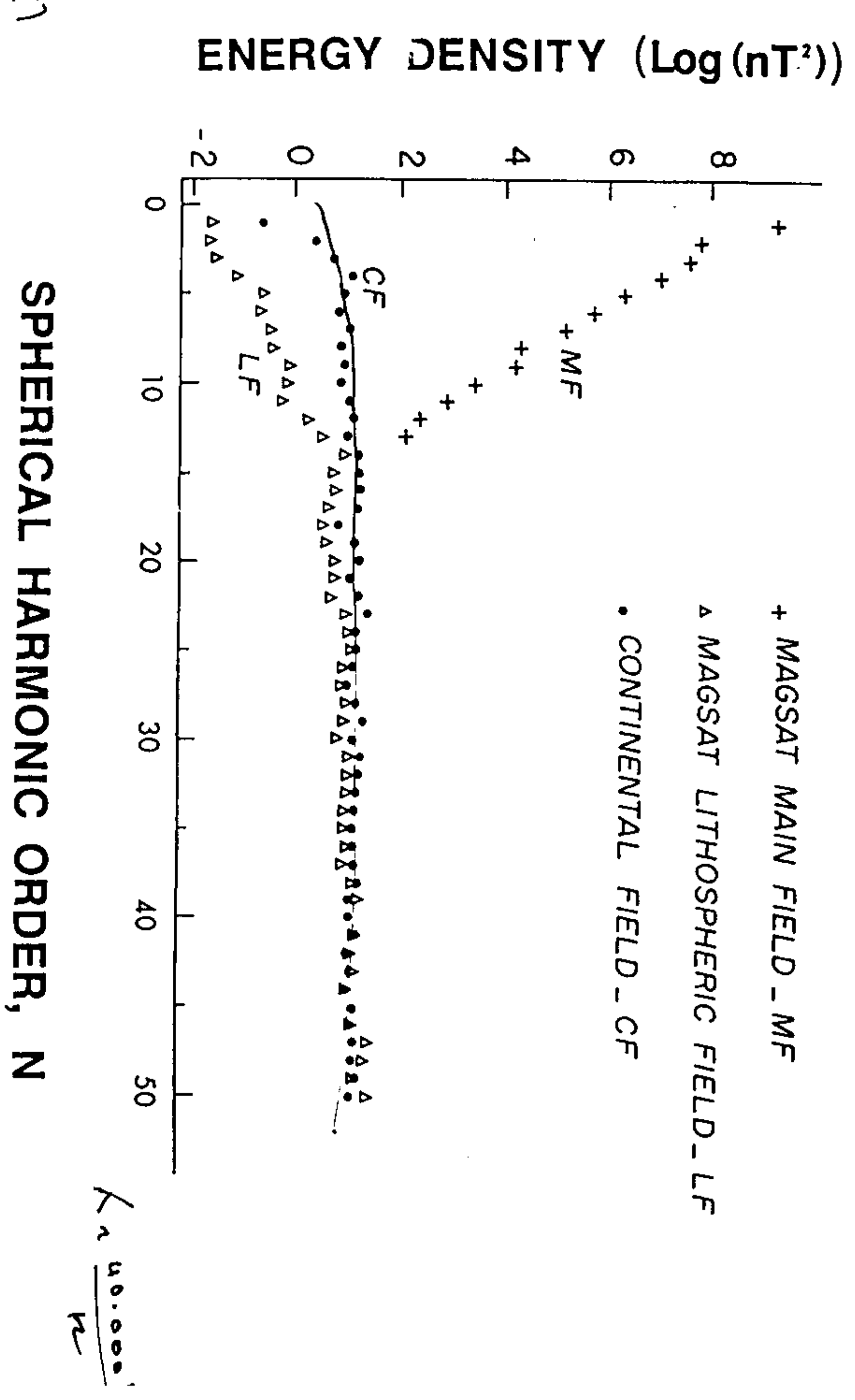

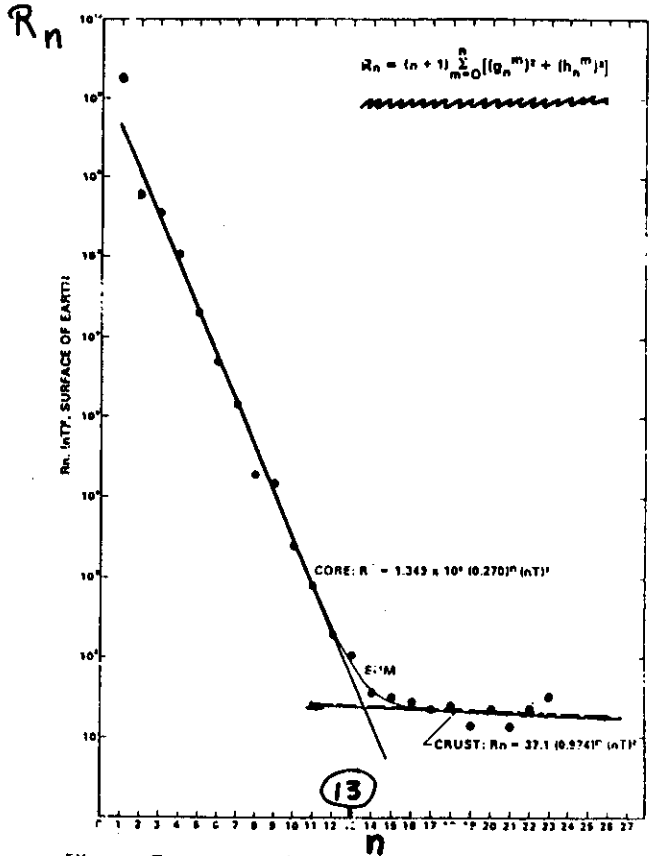

Fig. 2. Geomagnetic field spectrum. R_n is the total mean square contribution to the vector field by all harmonics of degree n. The curves are fit to the surface result.

Continuation through the mantle to the CMB.

1) $\sigma_m = 0$

$$\vec{B} = -\vec{\nabla} V \qquad \nabla^2 V = 0$$

$$\left(\frac{a}{r}\right)^{n+1} \longrightarrow \left(\frac{a}{b}\right)^{n+1} \sim \left(\frac{6.5}{3.6}\right)^{n+1} \sim$$

geometrical enhancement (attenuation)

$$W_n(b) = \left(\frac{a}{b}\right)^{2(n+2)} (n+1) \sum_{m=0}^{n} \left[(g_n^m)^2 + (h_n^m)^2 \right]$$

Map of B_r at the CMB.

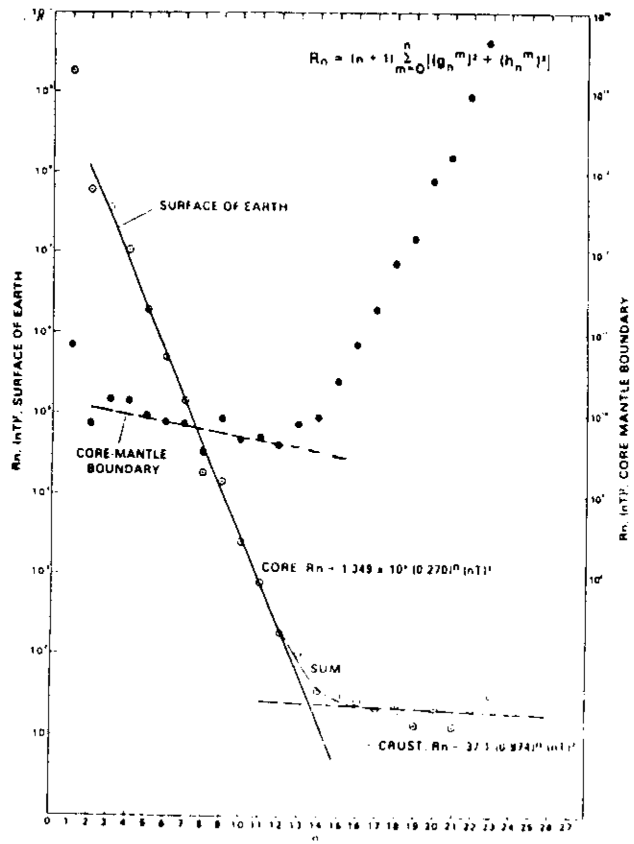

Figure 5 . Spectre d'énergie du champ géomagnétique calculé à la surface du globe et prolongé au noyau.

1980.0

1966.0

1955.5

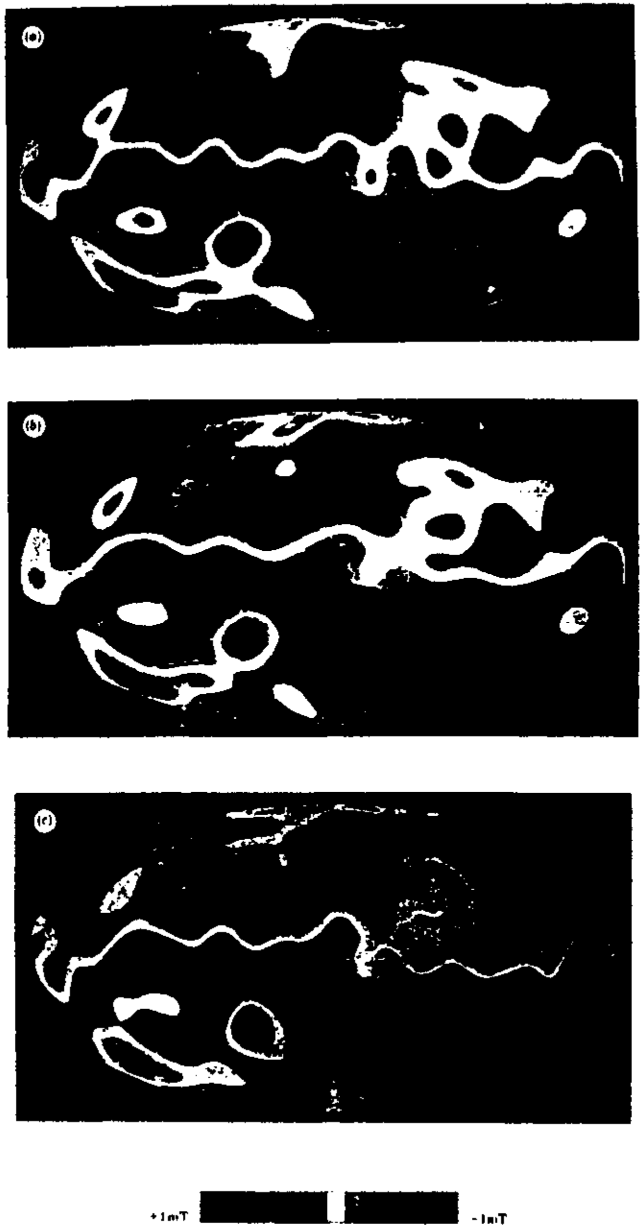

Figure 19 *a, b, c*. For description see opposite

2) $\sigma_m(r) \neq 0$

Computation of the electromagnetic field in the conducting mantle.

(Stix and Roberts, 1984; Backus, 1982; Benton and Whaler, 1983)

$\sigma_m \ll \sigma_c$

order 0 $\quad \vec{B} = \vec{B}_0 \quad \vec{J} = 0$

order 1 $\quad \vec{J}_1 = \sigma \vec{E}_1$

1) $\nabla \times \vec{E}_1 = -\dfrac{\partial \vec{B}_0}{\partial t} \longrightarrow \vec{E}_{1t}, \quad \vec{J}_{1t} = \sigma \vec{E}_{1t}$

2) $\vec{E}_1 = \vec{E}_{1t} + \vec{E}_{1p} = \vec{E}_{1t} - \vec{\nabla}\psi_1$

$$\text{II}\quad \left| \begin{array}{l} \Delta^2 \psi_1 + \dfrac{\sigma'}{\sigma} \dfrac{\partial \psi_1}{\partial r} = 0 \\[2ex] \left.\dfrac{\partial \psi_1}{\partial r}\right|_{r=b} = 0 \\[2ex] \psi_1(c+0) = -\Phi \qquad (\sigma_c\ \infty) \\[2ex] (\vec{u}\, B_{0r})_t = -\vec{n} \wedge \vec{\nabla}\Phi \end{array} \right.$$

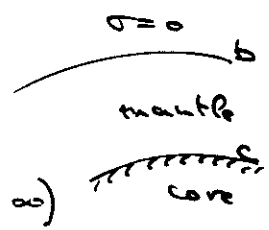

$\vec{u}, B_r$ known $\longrightarrow \Phi$ computed.

(needs an assumption on $\vec{u}$: $(\vec{u} B_r)_t$ undefined by S.V. data). Backus, 1986

Observations.

Main field: magnetic satellites

MAGSAT 1980

Oerstedt 1996

Secular variation.

magnetic observatories

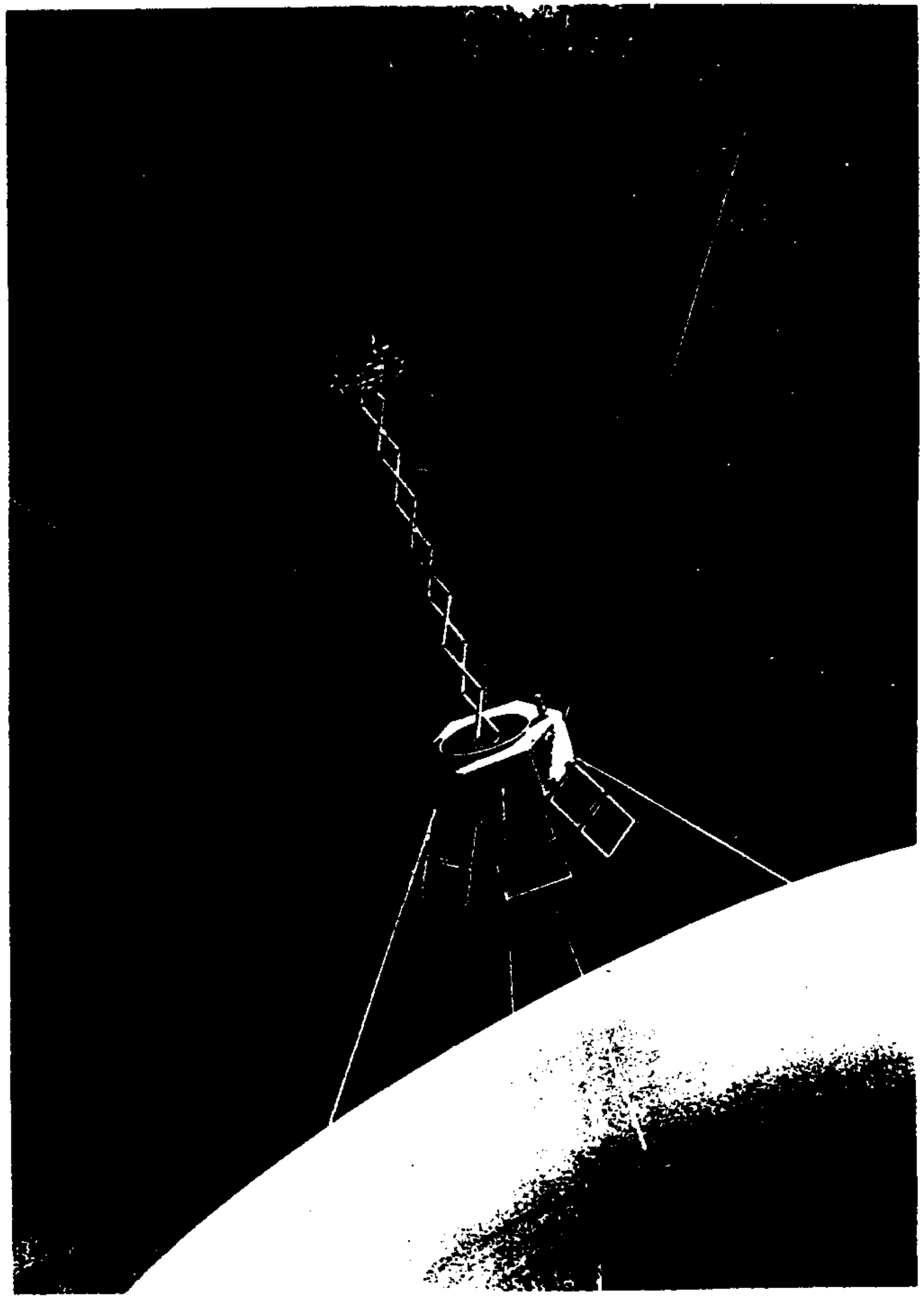

GRAVITY AND MAGNETIC EARTHPROBE STUDIES

(G A M E S)

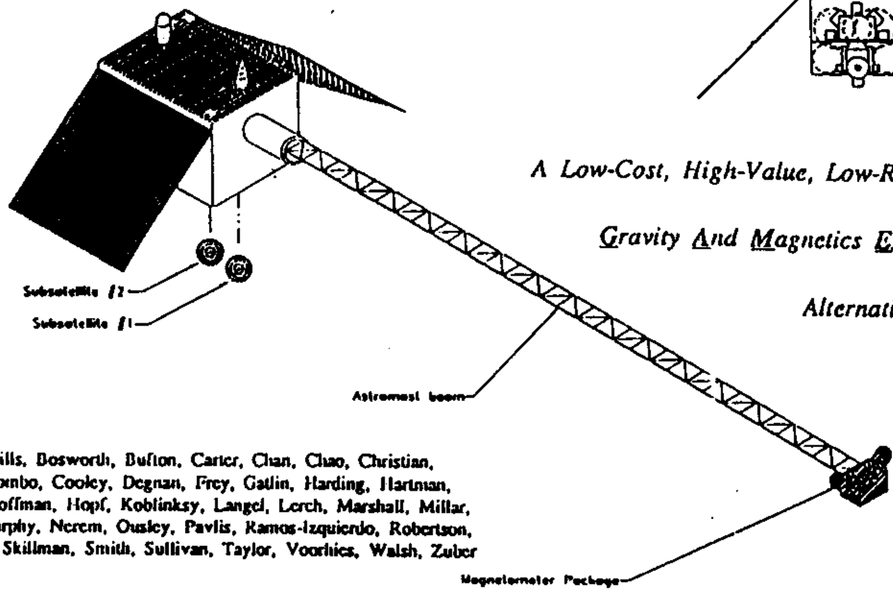

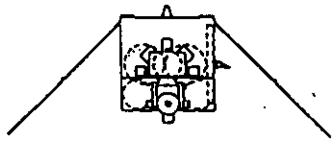

A Low-Cost, High-Value, Low-Risk

Gravity And Magnetics Experiment Satellite

Alternative to ARISTOTLES

Abshire, Bills, Bosworth, Bufton, Carter, Chan, Chao, Christian, Clark, Colombo, Cooley, Degnan, Frey, Gatlin, Harding, Hartman, Herrero, Hoffman, Hopf, Koblinksy, Langel, Lerch, Marshall, Millar, Moran, Murphy, Nerem, Ousley, Pavlis, Ramos-Izquierdo, Robertson, Rubincam, Skillman, Smith, Sullivan, Taylor, Voorhies, Walsh, Zuber

LABORATORY FOR TERRESTRIAL PHYSICS
GODDARD SPACE FLIGHT CENTER

3 November 1992